

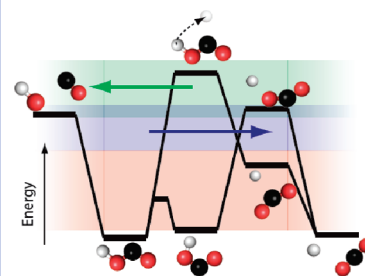
Dissociative Photodetachment Studies of Cooled HOCO^- Anions Revealing Dissociation Below the Barrier to $\text{H} + \text{CO}_2$

Christopher J. Johnson and Robert E. Continetti*

Department of Chemistry and Biochemistry and Department of Physics, University of California, San Diego, 9500 Gilman Drive, La Jolla, California 92093-0340

ABSTRACT Dissociative photodetachment of internally cold HOCO^- has been performed in a new cryogenically cooled photoelectron–photofragment coincidence apparatus, characterizing the HOCO potential energy surface in the Franck–Condon region determined by the anion. Three processes are observed in three distinct regions of this surface: detachment to stable HOCO , dissociative photodetachment to $\text{OH} + \text{CO}$, and dissociative photodetachment to $\text{H} + \text{CO}_2$. Relative to earlier work on internally hot anions, the $\text{H} + \text{CO}_2$ channel is significantly enhanced, with efficient dissociation to $\text{H} + \text{CO}_2$ unambiguously detected below calculated barriers in the $\text{OH} + \text{CO} \rightarrow \text{H} + \text{CO}_2$ reaction. This finding shows that an important low-energy pathway exists to the exit channel in this reaction, reinforcing the need for further refinement of this important potential energy surface and providing benchmarks for further theoretical efforts.

SECTION Dynamics, Clusters, Excited States



Considerable experimental and theoretical effort has focused on the hydroxyl formyl (HOCO) radical owing to its importance as a combustion reaction intermediate, particularly in the reaction of $\text{OH} + \text{CO} \rightarrow \text{H} + \text{CO}_2$.¹ Important recent contributions have been summarized elsewhere and will only briefly be outlined here. Kinetics studies have found that the thermal behavior of the rate coefficient for formation of $\text{H} + \text{CO}_2$ from $\text{OH} + \text{CO}$ is distinctly non-Arrhenius² and sensitive to vibrational excitation of the OH reactant,³ and several trans- HOCO vibrational modes have been characterized by direct absorption and matrix isolation techniques.^{4–7} Theoretical efforts have focused on the construction of an accurate potential energy surface (PES) for the HOCO intermediate and characterization of important stationary states^{8–12} to provide a basis for RRKM,^{13,14} quasiclassical^{11,10,15} and quantum dynamical^{16–20} studies of the reaction pathways on this surface as well as reactions of the HOCO radical with other species.²¹ However, direct experimental information about dynamics on the HOCO intermediate PES, particularly behavior in the well and near the barrier to the exit channel, is scarce due to difficulties in preparing this reactive intermediate.

In order to directly study this region of the PES, Clements et al. used photoelectron–photofragment coincidence (PPC) measurements of the dissociative photodetachment (DPD) of HOCO^- at 258 nm (4.80 eV) combined with ab initio calculations to probe the HOCO ground and excited PESs.²² These experiments measured the photoelectron kinetic energy (eKE) in coincidence with the center-of-mass translational energy release (E_T) for neutral dissociation, and found dissociation to both $\text{OH} + \text{CO}$ and $\text{H} + \text{CO}_2$ as well as stable HOCO . Lu et al.

extended these DPD experiments to 386 nm (3.21 eV) to obtain a better understanding of the dynamics occurring on the HOCO ground PES, and saw evidence for a tunneling mechanism for dissociation to $\text{H} + \text{CO}_2$.²³ However, these results also confirmed the presence of considerable internal excitation in the parent HOCO^- anions that resulted in uncertainties in the measured energetics and presented an alternate but less likely explanation to the tunneling hypothesis.

A new apparatus has been built, integrating a cryogenically cooled variant of a linear electrostatic ion beam trap (EIBT)²⁴ into an existing PPC spectrometer.²⁵ By storing ions in a cryogenic environment and carrying out PPC experiments on ions inside the trap, this method provides cold ions from a low-duty-cycle source but maintains the high duty cycle required for coincidence experiments. DPD of cold HOCO^- with 3.20 eV photons has been undertaken using this apparatus to gain a clearer understanding of the dynamics on the HOCO PES by removing the uncertainties in the anion internal energy. These new measurements show a considerable cooling effect, providing higher-resolution and less congested spectra and allowing the clear separation of contributions from the three observed processes: photodetachment to stable HOCO and DPD to both $\text{OH} + \text{CO}$ and $\text{H} + \text{CO}_2$. Additionally, as a result of the higher spectral resolution, these results further constrain the mechanism for the poorly understood $\text{H} + \text{CO}_2$ exit

Received Date: May 13, 2010

Accepted Date: May 20, 2010

Published on Web Date: June 07, 2010

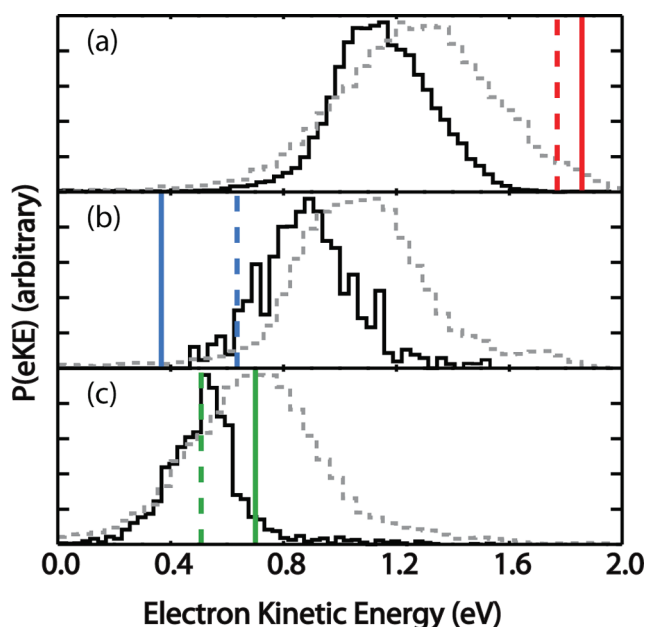


Figure 1. Channel-resolved photoelectron spectra for (a) $\text{HOCO} + e^-$, (b) $\text{H} + \text{CO}_2 + e^-$, and (c) $\text{OH} + \text{CO} + e^-$. Solid histograms indicate data from the current study; data from ref 23 are shown as dashed histograms. Vertical lines represent the maximum eKE expected from calculations in refs 22 and 9 for each channel.

channel, confirming dissociation of HOCO to $\text{H} + \text{CO}_2$ well below any calculated barrier to dissociation from the *cis*- or *trans*- HOCO^{9-12} well and suggesting an additional possible mechanism for this process.

Figure 1 summarizes the channel-resolved photoelectron spectra from “cold” (this work) and “hot” (Lu et al.) HOCO^- for each product channel with maximum expected electron kinetic energies ($e\text{KE}_{\text{max}} = h\nu - \text{adiabatic electron affinity (AEA)} - \text{calculated barrier height}$) in each channel shown for photodetachment of *cis*- (dashed) and *trans*- (solid) HOCO^- , respectively. The spectra from dissociative events correspond to events with two detected neutral particles and are separated into the two channels by enforcing conservation of momentum. Additionally, due to the large recoil velocity of H atoms in dissociation to $\text{H} + \text{CO}_2$, this spectrum is corrected for the detector acceptance function (DAF), which represents the probability of detecting both particles at a given kinetic energy release (KER) with respect to detector geometry and acquisition limitations.²⁶ This allows the recorded spectrum to be deconvolved to extract the true probability of detecting a photoelectron of given kinetic energy, or $P(e\text{KE})$. The HOCO and $\text{OH} + \text{CO}$ spectra are not affected by the DAF and are not corrected. Events leading to stable HOCO are separated by analyzing only single-particle events with less than 0.5 mm deviation from the ion beam center-of-mass, thereby reducing the contribution of events where only the heavy CO_2 fragment of dissociation to $\text{H} + \text{CO}_2$ is detected. Three distinct regions of the photoelectron spectrum are apparent, each corresponding to a specific process on the HOCO PES. Figure 1a shows a comparison of $P(e\text{KE})$ obtained from events leading to stable HOCO neutrals. Of primary importance in the cold spectrum is the fact that all observed photoelectrons

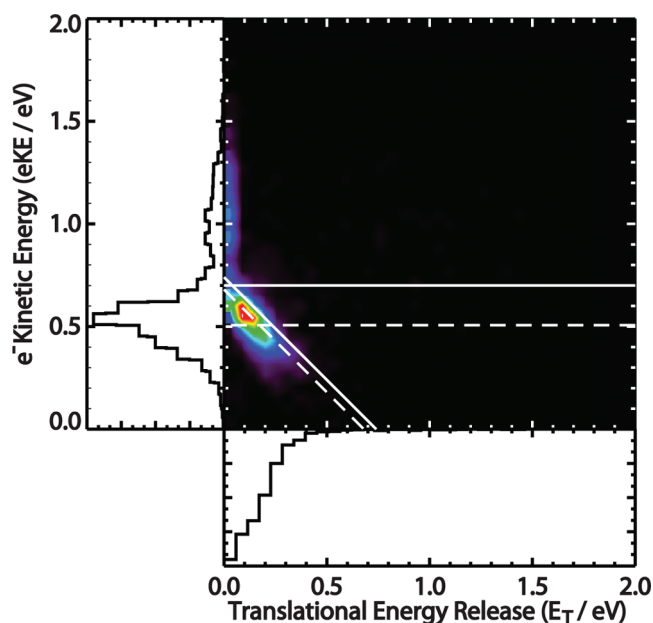


Figure 2. Coincidence spectrum for $\text{HOCO}^- + h\nu \rightarrow \text{OH} + \text{CO} + e^-$. Diagonal lines mark the maximum total energy available for DPD from *cis*- (dashed) and *trans*- (solid) HOCO^- based upon refs 22 and 9. Horizontal lines represent maximum eKEs for dissociation over barriers on the neutral surface following photodetachment from *cis*- (dashed) and *trans*- (solid) HOCO^- .

fall below the two limits, while the hot spectrum reveals photoelectrons of ~ 0.3 eV higher eKE, providing strong evidence that the ion precursors in the current experiment contain significantly lower internal energy. In the case of dissociation to $\text{H} + \text{CO}_2$, shown in Figure 1b, nearly all photoelectrons occur above the maximum predicted eKE for $\text{HOCO} \rightarrow \text{H} + \text{CO}_2$, indicating that all dissociation to the $\text{H} + \text{CO}_2$ limit occurs below the calculated barrier as observed by Lu et al. This spectrum too shows an overall shift toward lower eKE of ~ 0.3 eV, consistent with the removal of hot band contributions. Finally, Figure 1c shows the photoelectron spectrum for dissociation to $\text{OH} + \text{CO}$, which is similarly shifted to lower eKE by ~ 0.4 eV and significantly narrowed as a result of cooling of the precursor HOCO^- .

More detailed dynamical information can be extracted from the coincidence spectra for the $\text{H} + \text{CO}_2$ and $\text{OH} + \text{CO}$ channels. Figure 2 shows the correlation spectrum for dissociation to $\text{OH} + \text{CO}$ fragments, with a pair of diagonal lines representing the predicted total energy release ($E_{\text{TOT}} = e\text{KE} + \text{KER}$) for *cis*- and *trans*- HOCO^- isomers.²³ As in the $P(e\text{KE})$ spectra, these results also fall below the predicted E_{TOT} as would be expected of cooled ions. This spectrum is dominated by a narrow diagonal feature with full width at half-maximum (fwhm) of less than 0.1 eV. No vibrational excitation in either the OH or CO products is observed, consistent with photodetachment to a directly repulsive part of the PES.

Figure 3 shows the DAF-corrected coincidence spectrum for dissociation to $\text{H} + \text{CO}_2$. The diagonal lines in this spectrum again represent the predicted maximum E_{TOT} for each anion isomer, and again nearly all data falls below these limits. In this channel the diagonal band is quite broad, > 0.5 eV,

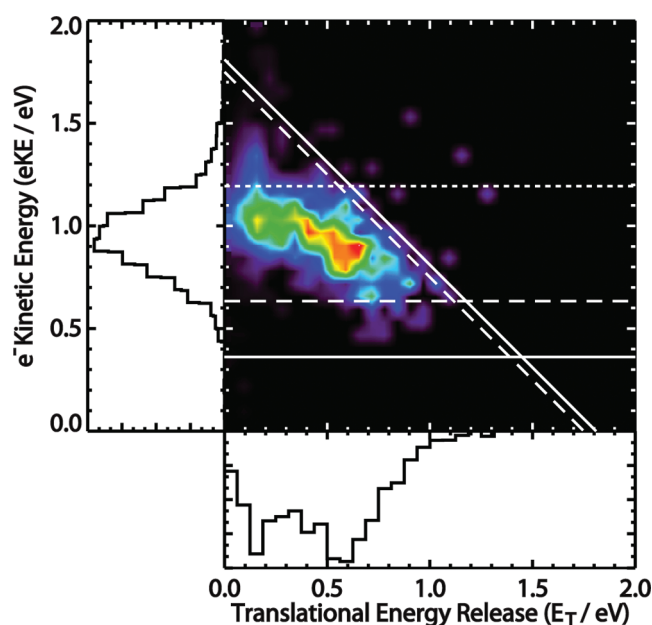


Figure 3. Coincidence spectrum for $\text{HOCO}^- + h\nu \rightarrow \text{H} + \text{CO}_2 + \text{e}^-$. Diagonal lines mark the maximum total energy available for DPD from *cis*-(dashed) and *trans*-(solid) HOCO^- based upon refs 22 and 9. Lower horizontal lines represent maximum eKEs for dissociation over barriers on the neutral surface following photodetachment from *cis*-(dashed) and *trans*-(solid) HOCO^- . The dashed horizontal line marks the maximum eKE allowing for isomerization to the C_{2v} HCO_2 structure.

indicating a high level of internal excitation in the CO_2 products. All dissociation is seen to occur above the eKE limits for both isomers; however, there appears to be a break in the diagonal band in the range of 1.1–1.2 eV, which results in a horizontal feature toward low KER. It is interesting to note that this feature nearly matches the maximum eKE expected for detachment from *trans*- HOCO^- to the C_{2v} HCO_2 isomer on the neutral surface.¹⁰ This suggests the possibility that detachment of HOCO^- to HOCO is followed by isomerization to HCO_2 prior to dissociation to $\text{H} + \text{CO}_2$, an alternative to direct tunneling through the dissociation barrier from the *cis*- HOCO isomer, which has been proposed but considered unlikely.^{1,9} The barrier to isomerization from *trans*- HOCO has been calculated to be much higher than the *cis*- HOCO barrier to $\text{H} + \text{CO}_2$, therefore this process would also require a tunneling mechanism given the calculated energetics, although H-atom migration is not unprecedented in systems of this size such as H_2CO .^{27,28}

Further information can be drawn from direct comparison of the new data to the previous hot data. In the case of photoelectron spectra, shifts to lower energy of > 0.3 eV are seen in all channels. This shift to lower energy is likely due not only to a reduction in internal energy of the anions, but also to the corresponding reduction in the extent of the Franck–Condon region sampled on the neutral PES resulting from the vibrationally cold anions and the resulting decrease in overlap of the anion and the neutral well. More strikingly, the eKE and coincidence spectra for the $\text{OH} + \text{CO}$ channel show huge differences, with dissociation occurring nearly entirely above the energetic limit in the hot data but nearly entirely below yet

near the limit for the cold data. The fact that there is relatively little signal in the hot spectrum that corresponds to the signal in the cold spectrum implies that this process was dominated by dissociation from vibrationally excited anions, an implication that is further strengthened by the fact that this channel also shows the largest shift to lower eKE of the three processes. Surprisingly, however, the $\text{H} + \text{CO}_2 + \text{e}^-$ coincidence spectrum shows only the removal of a higher energy feature found in the hot data, with the lower energy feature is virtually unchanged. The higher energy feature was previously assigned to hot bands, while the lower energy structure was proposed to result from tunneling through the barrier to $\text{H} + \text{CO}_2$ from cold anions, an assignment supported by this finding. This suggests that, in the Franck–Condon region determined by the cold anions, the neutral PES couples strongly to dissociation to $\text{H} + \text{CO}_2$ despite the apparent presence of high energetic barriers, but only weakly to dissociation to $\text{OH} + \text{CO}$. As the Franck–Condon region grows, however, the coupling to $\text{H} + \text{CO}_2$ apparently changes little, while the coupling to $\text{OH} + \text{CO}$ is greatly increased.

By examining the $P(\text{eKE})$ spectra in more detail, the relative contributions of *cis*- and *trans*-isomers to the observed DPD dynamics can be estimated to aid further analysis. Consideration of the $\text{OH} + \text{CO}$ channel in particular shows that the majority of the photoelectrons detected lie above the calculated barrier from the *cis*- HOCO well but below that for *trans*- HOCO , providing evidence that this process is dominated by dissociation from *trans*- HOCO . However, isomerization from *cis*- to *trans*- HOCO is facile in this part of the PES. In the case of detachment to stable HOCO , all photoelectrons occur below the limits for either isomer, with the observed maximum eKE lying close to the limit for *cis*- HOCO . It is therefore likely that the anion precursors are predominantly the lower-energy *cis*-isomers in this experiment.

An important metric for comparison to theoretical predictions and earlier experiments is the extraction of branching fractions, representing the relative probabilities of the three processes seen. By normalizing to unit area the $P(\text{eKE})$ spectra and scaling each to fit the total detected photoelectron signal, branching fractions may be estimated. In the bottom frame of Figure 4 the best fit using the three channel-resolved spectra is shown, giving a $\text{HOCO} : \text{H} + \text{CO}_2 : \text{OH} + \text{CO}$ branching fraction of 0.57 : 0.37 : 0.06, a significant change from those reported in earlier DPD studies^{22,23} and in stark contrast to calculated ratios which generally show production of the two dissociation channels in approximately equal low yields.¹⁹ This observation provides additional evidence that, in the Franck–Condon region, $\text{H} + \text{CO}_2$ is the dominant dissociation pathway. Energy-resolved branching fractions are plotted in the top frame of Figure 4, showing three clear energetic regions dominated by a single process, as well as transitions between each process. Unsurprisingly, in the lowest energy region on the PES the sole process seen is photodetachment to stable HOCO . However it is interesting to note that while the next highest region leads almost exclusively to $\text{H} + \text{CO}_2$, the highest region leads almost exclusively to $\text{OH} + \text{CO}$ even though both channels are energetically allowed. In fact, dissociation to $\text{H} + \text{CO}_2$ essentially ceases as soon as calculations predict that it becomes energetically allowed over the top of the

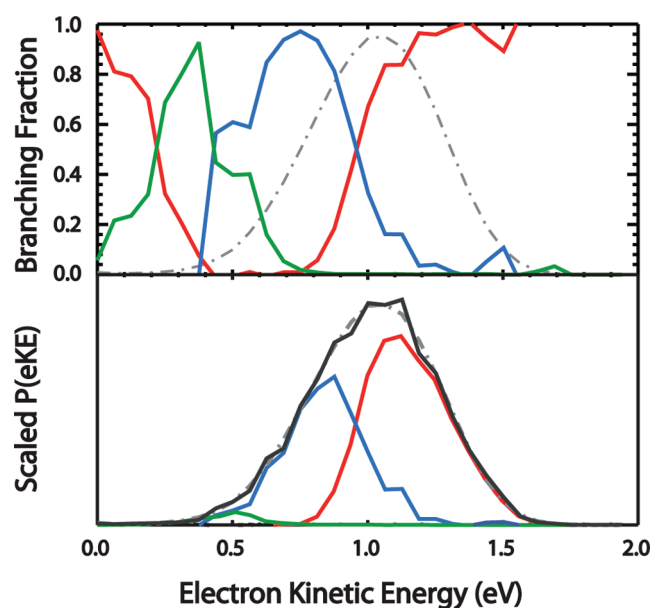


Figure 4. (Top) Branching fractions for the three channels as a function of eKE. Also shown is the total photoelectron yield for reference. (Bottom) Fit (solid black line) of scaled channel resolved spectra to the total photoelectron yield. In both figures, red indicates stable HOCO, blue indicates H + CO₂, green indicates OH + CO, and gray dot–dash lines indicates the total photoelectron spectrum.

barrier from *cis*-HOCO to H + CO₂. The transitions between these three distinct regions may also hold important clues about the interplay between these processes. Between the OH + CO channel and the H + CO₂ channel there is a ~0.1 eV wide area that leads to roughly equal amounts of OH + CO and H + CO₂, suggesting that low-energy collisions of OH and CO exploring this part of the PES find an efficient path to H + CO₂. Furthermore, the fact that dissociation to H + CO₂ is available well below the entrance channel indicates that collisional stabilization of the HOCO intermediate may greatly enhance the yield of H + CO₂ by cutting off the entrance channel and allowing the intermediate sufficient time to tunnel through the exit barrier. The transition between the H + CO₂ and HOCO regions contains, in principle, information about the tunneling probability as a function of energy and could provide an important test for more precise calculations of tunneling through the barrier to H + CO₂.

A clearer picture of the discrepancies between kinetic, theoretical, and previous experimental work in this laboratory can now be seen. The large branching ratio to H + CO₂ lying entirely below the barrier from either *cis*- or *trans*-isomers requires the existence of a yet-uncharacterized mechanism on this surface, which allows the system to bypass large energetic barriers as it dissociates to H + CO₂ at low energies. It may be that the portion of the neutral surface explored in this experiment is far enough away from the primary reaction pathway that this mechanism has been previously missed. Tunneling through the *cis*-barrier to H + CO₂ is commonly invoked as an explanation for the failure of calculations on *ab initio* surfaces to properly capture the reaction rates, and is supported by statistical calculations that include a correction

for tunneling.¹⁴ However, tunneling from *trans*-HOCO through the HCO₂ barrier appears not to have been studied in detail. The clear break in *P*(eKE) at the predicted energy for the HCO₂ isomer suggests that this possibility warrants further study. In either case, the present experiments provide unambiguous proof that further refinement of the exit channel region of the HOCO PES is necessary to fully understand this important combustion reaction.

EXPERIMENTAL METHODS

HOCO[−] anions were created in a pulsed discharge crossed by a 1 keV electron beam acting upon a pulsed supersonic expansion of a mixture of CH₄, CO, N₂O, and N₂ at 60 psi at 10 Hz. These ions were accelerated to 7 keV, rereferenced to ground in a fast high voltage switch, and mass selected by time-of-flight. HOCO anions at *m/e* = 45 were selected from the beam by an electrostatic chopper and injected into the EIBT, where they were stored for 990 ms in a cryogenic environment of approximately 20 K. Throughout the entire trapping cycle, this packet of ions was bunched and phase-locked to a 387 nm, 1.8 ps laser pulse from the 1 kHz Ti:Sa regenerative amplifier that intersected the ion bunch at the center of the trap. Photodetached electrons were collected in a velocity mapping time- and position-sensitive electron detector and neutral particles recoiled out of the trap onto a multiparticle time- and position-sensitive detector. Data was recorded on an event-by-event basis and stored on a PC for analysis at a later time. Calibration by O₂ photodetachment and O₄ DPD showed energy resolution of ~0.05 eV fwhm for photoelectrons and ~0.1 eV fwhm for neutral particles. No evidence for cooling or heating of anions during the 990 ms time scale of these measurements was seen in any spectrum, suggesting that the anion population is roughly in thermal equilibrium with the surrounding environment.

AUTHOR INFORMATION

Corresponding Author:

*To whom correspondence should be addressed. E-mail: rcontinetti@ucsd.edu.

ACKNOWLEDGMENT We acknowledge M. Rappaport and D. Zajfman for assistance in design of the cryogenic ion trap and the support of the DOE under Grant No. DE-FG03-98ER14879.

REFERENCES

- (1) Kudla, K.; Schatz, G.; Wagner, A. A Quasi-classical Trajectory Study of the OH + CO Reaction. *J. Chem. Phys.* **1991**, *95*, 1635–1647.
- (2) Fulle, D.; Hamann, H.; Hippler, H.; Troe, J. High Pressure Range of Addition Reactions of HO. II. Temperature and Pressure Dependence of the Reaction HO + CO ⇌ HOCO → H + CO₂. *J. Chem. Phys.* **1996**, *105*, 983–1000.
- (3) Brunning, J.; Derbyshire, D.; Smith, I.; Williams, M. Kinetics of OH(*v* = 0, 1) and OD(*v* = 0, 1) with CO and the Mechanism of the OH + CO Reaction. *J. Chem. Soc., Faraday Trans. 2* **1988**, *84*, 105–119.
- (4) Jacox, M. The Vibrational Spectrum of the *trans*-HOCO Free-Radical Trapped in Solid Argon. *J. Chem. Phys.* **1988**, *88*, 4598–4607.

- (5) Sears, T.; Fawzy, W.; Johnson, P. Transient Diode-Laser Absorption-Spectroscopy of the ν_2 Fundamental of *trans*-HOCO and DOCO. *J. Chem. Phys.* **1992**, *97*, 3996–4007.
- (6) Petty, J.; Moore, C. Transient Infrared-absorption Spectrum for the ν_1 Fundamental of *trans*-HOCO. *J. Mol. Spectrosc.* **1993**, *161*, 149–156.
- (7) Forney, D.; Jacox, M.; Thompson, W. Infrared Spectra of *trans*-HOCO, HCOOH^+ , and HCO_2^- Trapped in Solid Neon. *J. Chem. Phys.* **2003**, *119*, 10814–10823.
- (8) Schatz, G.; Fitzcharles, M.; Harding, L. State-to-State Chemistry with Fast Hydrogen-Atoms - Reaction and Collisional Excitation in $\text{H} + \text{CO}_2$. *Faraday Discuss.* **1987**, *84*, 359–369.
- (9) Yu, H.; Muckerman, J.; Sears, T. A Theoretical Study of the Potential Energy Surface for the Reaction $\text{OH} + \text{CO} \rightarrow \text{H} + \text{CO}_2$. *Chem. Phys. Lett.* **2001**, *349*, 547–554.
- (10) Lakin, M.; Troya, D.; Schatz, G.; Harding, L. A Quasiclassical Trajectory Study of the Reaction $\text{OH} + \text{CO} \rightarrow \text{H} + \text{CO}_2$. *J. Chem. Phys.* **2003**, *119*, 5848–5859.
- (11) Valero, R.; Van Hemert, M.; Kroes, G. Classical Trajectory Study of the HOCO System Using a New Interpolated *Ab Initio* Potential Energy Surface. *Chem. Phys. Lett.* **2004**, *393*, 236–244.
- (12) Song, X.; Li, J.; Hou, H.; Wang, B. *Ab Initio* Study of the Potential Energy Surface for the $\text{OH} + \text{CO} \rightarrow \text{H} + \text{CO}_2$ Reaction. *J. Chem. Phys.* **2006**, *125*, 094301.
- (13) Golden, D.; Smith, G.; McEwen, A.; Yu, C.; Eiteneer, B.; Frenklach, M.; Vaghjiani, G.; Ravishankara, A.; Tully, F. $\text{OH}(\text{OD}) + \text{CO}$: Measurements and an Optimized RRKM Fit. *J. Phys. Chem. A* **1998**, *102*, 8598–8606.
- (14) Chen, W.; Marcus, R. On the Theory of the CO plus OH Reaction, Including H and C Kinetic Isotope Effects. *J. Chem. Phys.* **2005**, *123*, 094307.
- (15) Bradley, K.; Schatz, G. A Quasiclassical Trajectory Study of $\text{H} + \text{CO}_2$: Angular and Translational Distributions, and OH Angular Momentum Alignment. *J. Chem. Phys.* **1997**, *106*, 8464–8472.
- (16) Yu, H.; Muckerman, J. Quantum Dynamics of the Photoinitiated Unimolecular Dissociation of HOCO. *J. Chem. Phys.* **2002**, *117*, 11139–11145.
- (17) Valero, R.; McCormack, D.; Kroes, G. New Results for the $\text{OH}(\nu = 0, j = 0) + \text{CO}(\nu = 0, j = 0) \rightarrow \text{H} + \text{CO}_2$ Reaction: Five- and Full-Dimensional Quantum Dynamical Study on Several Potential Energy Surfaces. *J. Chem. Phys.* **2004**, *120*, 4263–4272.
- (18) Garcia, E.; Saracibar, A.; Zuazo, L.; Lagana, A. A Detailed Trajectory Study of the $\text{OH} + \text{CO} \rightarrow \text{H} + \text{CO}_2$ Reaction. *Chem. Phys.* **2007**, *332*, 162–175.
- (19) Zhang, S.; Medvedev, D. M.; Goldfield, E. M.; Gray, S. K. Quantum Dynamics Study of the Dissociative Photodetachment of HOCO^- . *J. Chem. Phys.* **2006**, *125*, 164312.
- (20) He, Y.; Goldfield, E.; Gray, S. Quantum Dynamics of Vibrationally Activated $\text{OH}-\text{CO}$ Reactant Complexes. *J. Chem. Phys.* **2004**, *121*, 823–828.
- (21) Yu, H.-G.; Poggi, G.; Francisco, J. S.; Muckerman, J. T. Energetics and Molecular Dynamics of the Reaction of HOCO with HO_2 Radicals. *J. Chem. Phys.* **2008**, *129*, 214307.
- (22) Clements, T.; Continetti, R.; Francisco, J. Exploring the $\text{OH} + \text{CO} \rightarrow \text{H} + \text{CO}_2$ Potential Surface via Dissociative Photodetachment of HOCO^- . *J. Chem. Phys.* **2002**, *117*, 6478–6488.
- (23) Lu, Z.; Hu, Q.; Oakman, J. E.; Continetti, R. E. Dynamics on the HOCO Potential Energy Surface Studied by Dissociative Photodetachment of HOCO^- and DOCO^- . *J. Chem. Phys.* **2007**, *126*, 194305.
- (24) Dahan, M.; Fishman, R.; Heber, O.; Rappaport, M.; Altstein, N.; Zajfman, D.; Van Der Zande, W. A New Type of Electrostatic Ion Trap for Storage of Fast Ion Beams. *Rev. Sci. Instrum.* **1998**, *69*, 76–83.
- (25) Hanold, K.; Luong, A.; Clements, T.; Continetti, R. Photoelectron–Multiple-Photofragment Coincidence Spectrometer. *Rev. Sci. Instrum.* **1999**, *70*, 2268–2276.
- (26) Continetti, R.; Cyr, D.; Osborn, D.; Leahy, D.; Neumark, D. Photodissociation Dynamics of the N_3 Radical. *J. Chem. Phys.* **1993**, *99*, 2616–2631.
- (27) Townsend, D.; Lahankar, S.; Lee, S.; Chambreau, S.; Suits, A.; Zhang, X.; Rheinecker, J.; Harding, L.; Bowman, J. The Roaming Atom: Straying From the Reaction Path in Formaldehyde Decomposition. *Science* **2004**, *306*, 1158–1161.
- (28) Goncharov, V.; Lahankar, S. A.; Farnum, J. D.; Bowman, J. M.; Suits, A. G. Roaming Dynamics in Formaldehyde- d_2 Dissociation. *J. Phys. Chem. A* **2009**, *113*, 15315–15319.